Electronic Supplementary Material (ESI) for Lab on a Chip.

Supporting Information

Dynamic investigation of zein-based degradable and hemocompatible coatings for drug-eluting stents: a microfluidic approach

Martina Lenzuni [a,b], Silvio Bonfadini [c], Luigino Criante [c], Filippo Zorzi [c,d], Maria Summa [e], Rosalia Bertorelli [e], Giulia Suarato [a,e,† *], Athanassia Athanassiou [a*†]*

a Smart Materials Group, Istituto Italiano di Tecnologia, via Morego 30, Genoa, Italy

b Department of Computer Science, Bioengineering, Robotics and Systems Engineering, University of Genoa, via Opera Pia 13, Genoa, Italy

c Center for Nano Science and Technology @ PoliMi, Istituto Italiano di Tecnologia, via Pascoli 70/3, Milan, Italy

d Department of Physics, Politecnico di Milano, Piazza Leonardo da Vinci, 32, Milano, Italy

e Translational Pharmacology, Istituto Italiano di Tecnologia, via Morego 30, Genoa, Italy

† co-last authors

*corrisponding authors: martina.lenzuni@iit.it, athanassia.athanassiou@iit.it, giulia.suarato@ieiit.cnr.it.

(a)

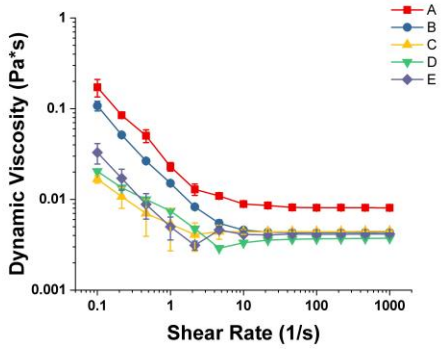

Table S1. Dynamic viscosity for water-glycerol solutions with and without urea.

	Water (wt%)	Glycerol (wt%)	Urea (wt%)	Dynamic Viscosity (mPa*s)
A	44.2	55.8	-	8.9
B	54.3	45.7	-	4.6
C	44.1	34.5	21.4	4.4
D	45.6	28.8	25.6	3.3
E	44.8	32.8	22.4	4.1

Table S2. Comparison between ion concentrations of SBF_ws and human blood plasma.

Ion	Na^+	K^+	Mg^{2+}	Ca^{2+}	HPO_4^{2-}	HCO_3^-	Cl^-	SO_4^{2-}	Buffer agent
Human Blood Plasma (mM)	142	5	1.5	2.5	1	27	103	0.5	-
SBF_ws (mM)	142	5	1.5	2.5	1	27	125	0.5	Tris

Figure S1. Simulated blood fluid (SBF) solutions. Relationships between dynamic viscosity and shear rate for water/glycerol (wg) and water/glycerol/urea (wgu) solutions are shown in figure (a). Table S1 shows the measured dynamic viscosities for the prepared solutions, while Table S2 compares the ion concentrations of SBF_ws and those of human blood plasma.

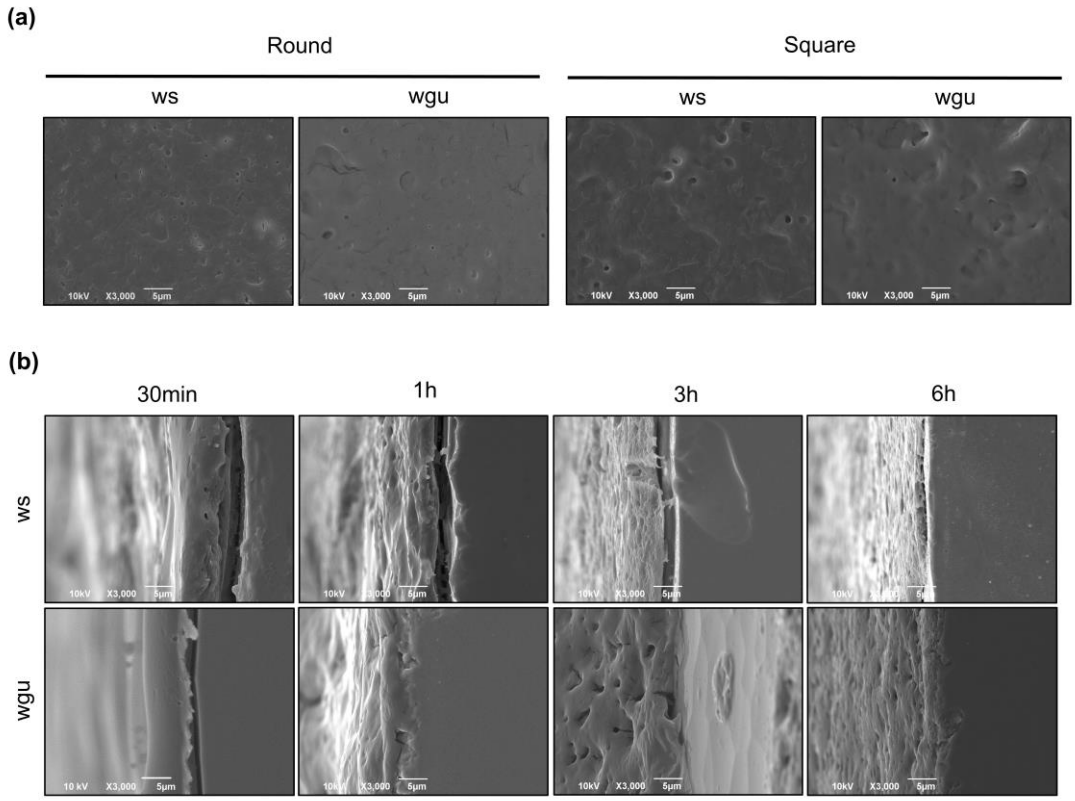

Figure S2. Additional SEM images of degrading coated channels. SEM micrographs of degradation coating at time t = 60 minutes (a). Morphological changes observed on the edge (b) of the coated channels during the degradation process. Representative SEM images of the square and round chips were taken at different time points (from 30 minutes to 6 hours).

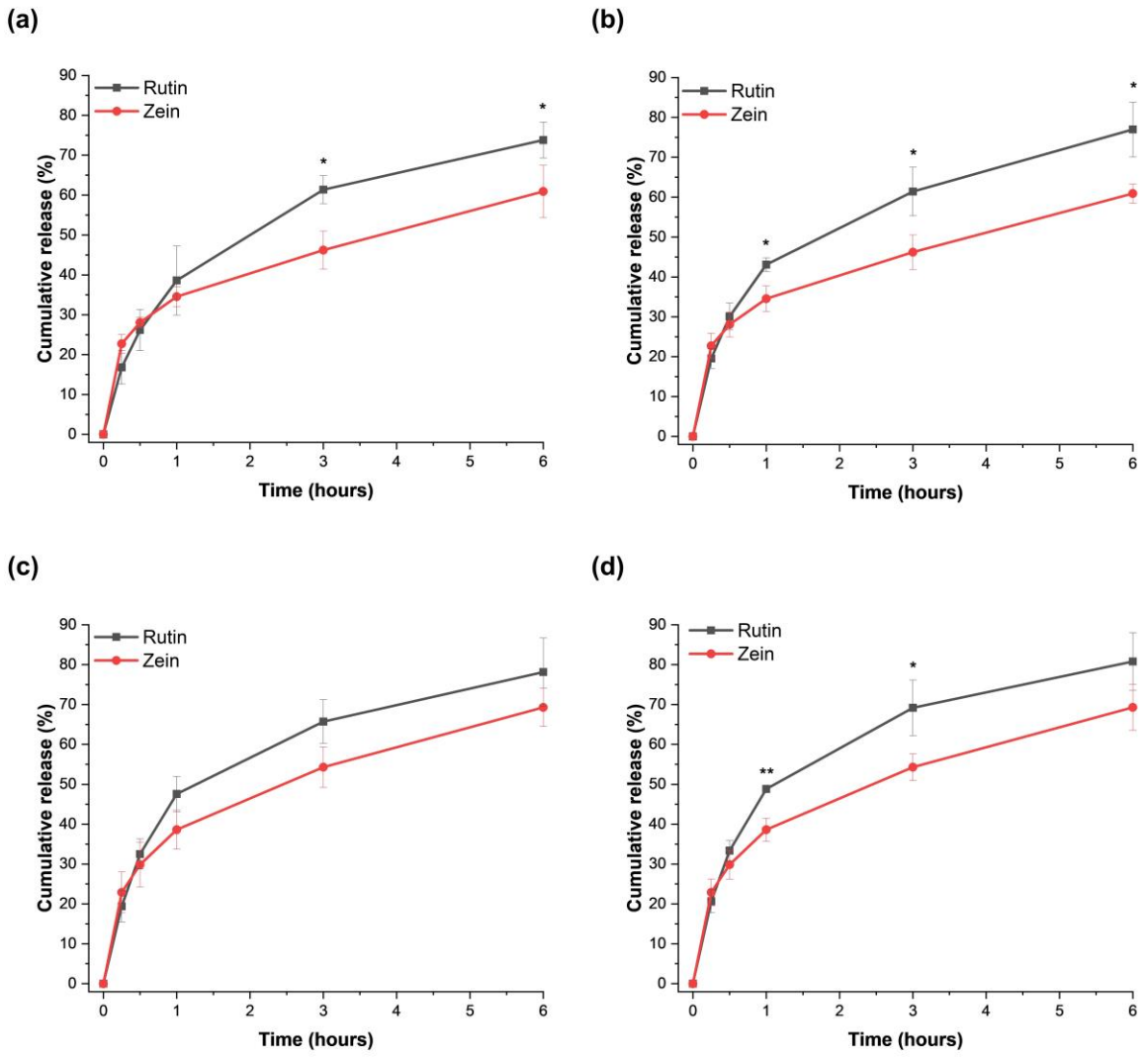

Figure S3. Comparison between drug and polymer release from ZR-coated microfluidic chips. Zein mass and rutin release from round (a, b) and square (c, d) channels in the presence of continuous SBF_wgu (a, c) and SBF_ws (b, d) flows. Data are presented as mean ± SD (n = 3), which were statistically analyzed using Student's t-test. * $p < 0.05$, ** $p < 0.01$.

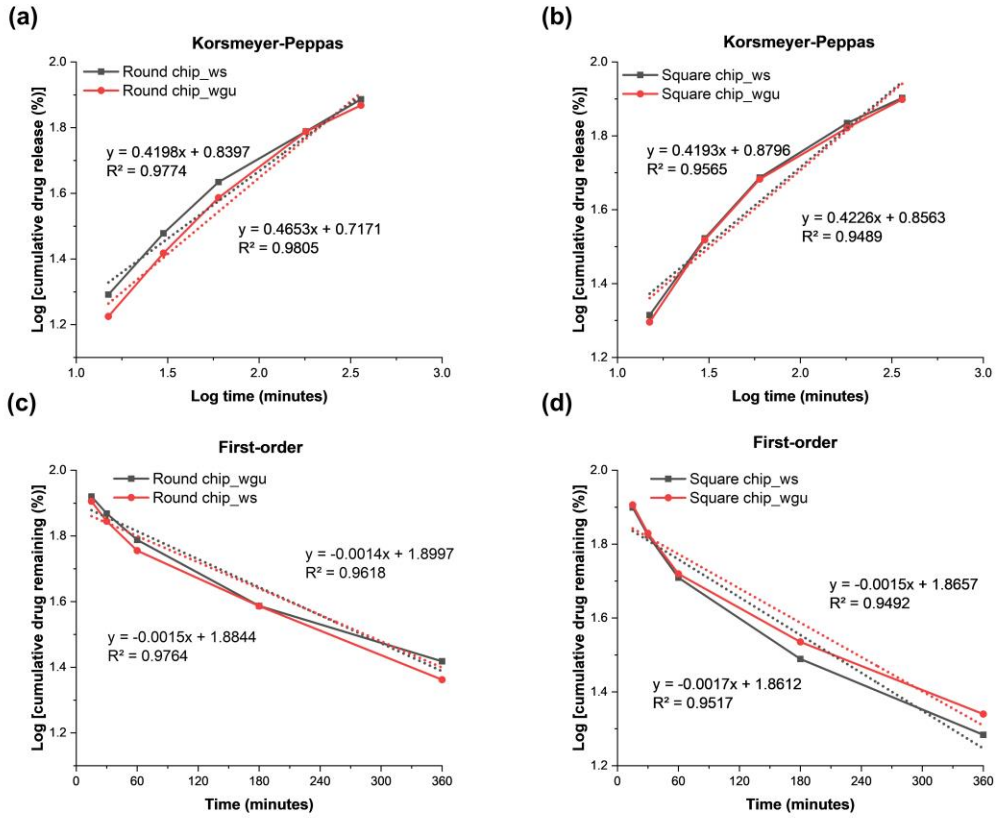

Table S3: Mathematical model fitting values obtained from rutin release kinetics for different time periods

CROSS-SECTION	SBF TYPE	ANALYZED TIME (min)	ZERO ORDER	FIRST ORDER	HIGUCHI	KORSMEYER-PEPPAS		HIXSON-CROWELL
			r^2	r^2	r^2	r^2	n	r^2
Round	ws	0 - 60	0.9835	0.9935	**0.9986**	0.9974	0.5696	0.9907
Round	ws	60 - 360	0.974	0.9989	0.9983	**1**	0.3237	0.9942
Round	wgu	0 - 60	0.9881	0.9954	**0.9997**	0.9986	0.6004	0.9934
Round	wgu	60 - 360	0.9222	0.9729	0.974	**0.9871**	0.3672	0.9583
Square	ws	0 - 60	0.9825	0.9948	**0.9983**	0.9958	0.6204	0.9915.
Square	ws	60 - 360	0.9282	0.9819	0.9775	**0.9923**	0.2843	0.9691
Square	wgu	0 - 60	0.9776	0.992	**0.9965**	0.9924	0.6472	0.988
Square	wgu	60 - 360	0.9512	0.9903	0.9897	**0.9982**	0.2785	0.9804

Figure S4. Rutin release fitting profiles. Rutin release profiles were adjusted to different mathematical models, among which the Korsmeyer-Peppas (a, b) and First-order (c, d) models resulted to be the most

accurate. These models could help estimate the mechanism of rutin release from round (a, c) and square (b, d) coated channels with different flow fluids. Table S3 presents the correlation coefficients (r^2) from drug release profiles obtained by analyzing different time periods with different mathematical models. Bold numbers indicate the highest r^2 values for each type of experiment.

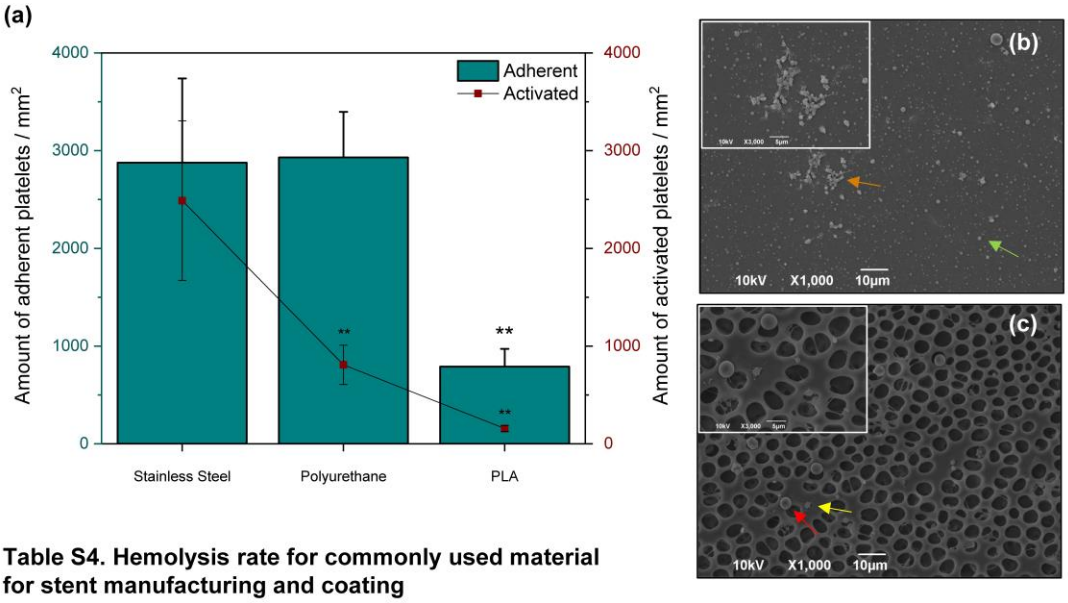

Table S4. Hemolysis rate for commonly used material for stent manufacturing and coating

Sample surface	Hemolysis Rate (%)
Normal saline (negative control)	0
Distilled water (positive control)	100
Stainless Steel	1.20 ± 0.54
Polyurethane	22.08 ± 1.61
PLA	3.00 ± 0.21

Figure S5. Hemocompatibility tests for commonly used materials for stent coatings. The amount of adhered and activated platelets on different substrates is shown in figure (a), while representative SEM images and magnified insets show platelets on polyurethane (b) and PLA (c)-coated substrates. Data are presented as mean ± SE, which were statistically analyzed using one-way ANOVA followed by post hoc Tukey's test (** $p < 0.01$). Arrows indicate red blood cells (red), resting platelets (green), activated platelets (yellow), and aggregated platelets (orange). Table S4 reports the hemolysis rate of reference materials used for stent manufacturing and coating. Data are presented as mean ± SE.

Figure S5 shows the adhesion and morphology of platelets on the reference sample surfaces (PU and PLA) after contact with the whole blood. The average number of adherent and activated platelets per mm^2 were 2930 and 808 for the PU coating and 790 and 156 for the PLA coating. The latter shows a similar behavior compared to what observed by Kim *et al.* with PLGA-coated substrate (~875 adherent platelets/mm^2) [1]. The quantities of adherent cells on both PU and SS samples were significantly higher than those on PLA and zein-based samples, with a high degree of spreading and aggregation. In particular, severe platelet aggregation was observed on the PU-coated surface (Figure S5(b)), indicating significant activation and poor hemocompatibility of the material, as already reported for other types of polyurethanes in the literature [2]. Compared to the other samples, the number of erythrocytes increased when in contact with the PLA surface (Figure S5(c)), probably due to the morphology and the specific surface area of this synthetic polymer, which allows more cells to adhere, as already reported by Ji *et al* [3].

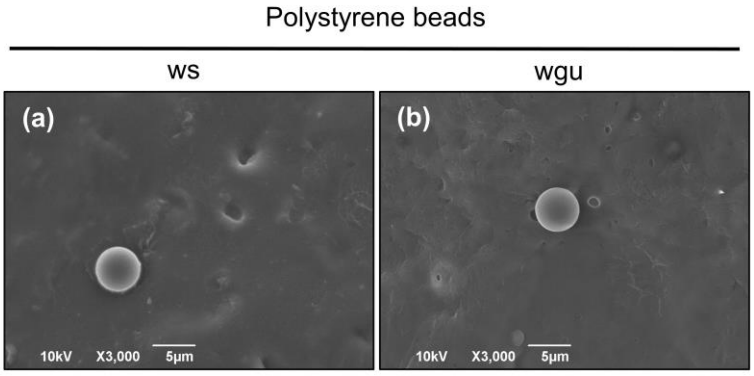

Figure S6. Polystyrene beads adhesion. SEM images of ZR-coated channels were acquired after a 30 min flow of PS beads (5-μm diameter, mimicking a red blood cell) dispersed in SBF_ws (a) and SBF_wgu (b).

Although such a particle model does have its limitations, and it clearly does not recreate all the complexities involved in an *in vivo* environment, it can provide a useful indication of possible adhesion

events that may occur at the zein/liquid interface. The particles shown in Figure S6 likely adhere to the polymer coating due to Van der Waals, hydrophobic and electrostatic interactions. The zeta potential of the 5-µm PS particles measured -4.6 ± 0.08 mV when dispersed in SBF_wgu and -7.4 ± 1.1 mV when resuspended in SBF_ws. This difference could be explained by the presence of some glycerol and urea molecules on the particles surface, which could lead to electric-double layer compression and, therefore, slightly modify the zeta potential value [4, 5]. No difference in the number of adherent particles can be noticed when qualitatively comparing the images obtained with PS beads dispersed in the two SBFs.

REFERENCES

1. J. H. Kim, N. R. Ko, B.-Y. Jung and I. K. Kwon, *Macromolecular Research*, 2016, **24**, 931-939.
2. B. Butruk-Raszeja, M. Trzaskowski and T. Ciach, *J Biomater Appl*, 2015, **29**, 801-812.
3. X. Ji, W. Yang, T. Wang, C. Mao, L. Guo, J. Xiao and N. He, *Journal of Biomedical Nanotechnology*, 2013, **9**, 1672-1678.
4. A. McKenzie, R. Hoskins, T. Swift, C. Grant, and S. Rimmer, *ACS Applied Materials & Interfaces*, 2017, **9**, 7577-7590.
5. F. C. Silva, L. C. B. Lima, C. Viseras, J. A. Osajima, J. M. da Silva Júnior, R. L. Oliveira, L. R. Bezerra and E. C. Silva-Filho, *Molecules (Basel, Switzerland)*, 2019, **24**, 3525.